Hindawi
Journal of Nanomaterials
Volume 2019, Article ID 8318260, 7 pages
https://doi.org/10.1155/2019/8318260

Research Article

Effect of Cellulose Nanocrystals on the Properties of Cement Paste

Qiaoling Liu,[1,2] **Yujiao Peng**,[1,2] **Long Liang**,[1,2] **Xiaobin Dong**,[3] **and Hancai Li**[1,2]

[1]*School of Civil Engineering, Shandong Jianzhu University, Jinan 250101, China*
[2]*Key Laboratory of Building Structural Retrofitting and Underground Space Engineering of Ministry of Education, Jinan 250101, China*
[3]*School of Materials Science and Engineering, Shandon Jianzhu University, Jinan 250101, China*

Correspondence should be addressed to Qiaoling Liu; lql263@163.com

Received 20 July 2019; Revised 24 September 2019; Accepted 3 October 2019; Published 16 December 2019

Guest Editor: Yunpan Ying

The effect of the addition of cellulose nanocrystals (CNCs) on the properties of cement pastes is studied herein. The compressive strength of CNC/cement paste was investigated under the curing conditions defined in this study. Two-dimensional micrographs and pore size distributions were obtained by scanning electron microscopy, X-ray computed tomography (XCT), and nitrogen adsorption. The addition of CNCs was found to significantly enhance the mechanical properties of cement pastes with a rapid decrease in temperature and humidity. XCT and nitrogen adsorption analyses show that the addition of CNCs leads to a refinement of the pore structure in the cement matrix. Almost no hydration products, including C-S-H, are formed in the cement matrix without CNCs under extreme conditions. This is in contrast with the results for the cement paste with 0.5% CNCs.

1. Introduction

In recent decades, research on nanocrystals including organic and inorganic materials has become a promising topic. Owing to their excellent properties, nanocrystals have been applied in medicine, catalysis, biology, and composites. However, most nanocrystals have been prepared by chemical synthesis, such as SiC nanocrystals, ZnO nanocrystals, GaAs nanocrystals, and poly (butylene carbonate). Although the size and shape of synthetic nanocrystals can be controlled when compared to CNCs, the preparation of nanocrystals will lead to the destruction of resources and result in environmental pollution [1–9]. However, CNCs are manufactured from natural sources such as trees and plants. Thus, CNCs have developed rapidly in recent years as nanofibers that are environmentally friendly and renewable. Furthermore, they have many extraordinary properties when compared to other nanofibers, such as an ultrafine diameter, low density, and low cost. They also show good water dispersibility without the need of any modification or the addition of any surfactant [10, 11].

Cellulose nanocrystals (CNCs) have become a potential nanofiber material that can improve the properties of cement paste. Previous research has shown that the addition of CNCs can prevent microcracking and improve the mechanical properties of cement paste [12–16]. An addition of only 0.2% volume of CNCs can increase the flexural strength of cement by approximately 30% [15]. After ultrasonication, this can reach up to 50% [16]. Furthermore, the degree of hydration (DOH) of cement pastes can be improved by employing CNCs. Short-circuit diffusion mechanism is more dominant than steric stabilization; this explains the increase in DOH caused by CNCs [15]. Cao et al. [16] found that when a simulated pore solution of cement paste replaces deionized water, CNCs will be more probable to agglomeration at a lower concentration. This shows that the dispersion of CNCs plays a key role in improving the flexural strength of the cement paste, particularly at a high concentration of CNCs.

This study investigated the tremendous influence of CNCs on cement pastes under the curing conditions defined, which is detrimental to cement hydration.

2. Materials and Methods

2.1. Materials. Ordinary Portland cement is used in this study. Table 1 lists the chemical composition and physical

Table 1: Chemical composition and physical properties of cement.

Chemical composition (wt.%)							Special surface area, Blaine ($m^2 \cdot kg^{-1}$)	Compressive strength (MPa)
CaO	SiO_2	Al_2O_3	Fe_2O_3	MgO	SO_3	Ignition loss		
63.6	21.2	3.2	3.0	1.0	2.5	2.3	385	52.1

wt.% represents mass fraction.

Table 2: Mixture proportions.

No.	Cement/g	CNCs/g	Water/g
C1	100	0	50
C2	100	0.2	50
C3	100	0.5	50
C4	100	0.2	40

properties of this type of cement. The CNC materials are manufactured by the laboratory of Nanjing Forestry University. The CNCs are extracted from cotton cellulose fibers. Firstly, the microcrystalline cellulose of cotton is hydrolyzed with 64 wt.% H_2SO_4, after which the solution is diluted with distilled water and the suspension is centrifuged. After repeating the dilution and centrifugation, the precipitates collected are further dialyzed with distilled water from a dialysis tube (Biosharp; molecular mass cutoff = 14400, USA) until its pH becomes 7.0. Subsequently, the CNC suspension is ultrasonically dispersed for 30 min. Therefore, the CNC material is a suspension at a concentration of 1.1 wt.%. The width and length of CNCs are 4–9 nm and 100–400 nm, respectively.

2.2. Mixing and Specimen Preparation. Table 2 shows the proportion of cement paste mixtures. The cement pastes are created in a rotary mixer. Cement is added first, after which water and the CNC solution are introduced and the pastes are mixed. The pastes are then poured into 30 × 30 × 30 mm molds. All samples are demolded after 24 h and then cured at 20 ± 2°C and a relative humidity (RH) ≥ 95% for 7 d. Subsequently, these samples were moved to a curing room and treated at 4 ± 2°C and RH of 55 ± 5% for 21 d.

2.3. Testing. The micromorphology of CNCs in water was observed by transmission electron microscopy (TEM) (JEM-1400, Japan). The compressive strength of cement pastes was measured at defined ages. To study the 2D microstructure and pore size distribution of cement pastes, the samples were crushed into pieces and soaked in ethanol for 48 h to stop the hydration of cement. The samples were then dried in an oven at 45 ± 5°C for 48 h, and the dried samples were stored in a dryer. Scanning electron microscopy (SEM) was used to characterize the 2D microstructure of the samples. The samples, after curing for a defined number of days, were cut into 1.5 ± 0.5 cm thick slices; central cylinders with a diameter of 1 cm were obtained using a water saw. Then, three-dimensional (3D) images were obtained, and the defect distributions of cement pastes without any prior damaging preparation were tested via X-ray computed tomography (XCT; Xradia 510 Versa, Zeiss, Germany). The voltage and current of the X-ray tubes were 80 kV and 87 μA, respectively. The pore size distributions of the cement paste were determined by nitrogen adsorption via the Barrett–Joyner–Halenda (BJH) analysis.

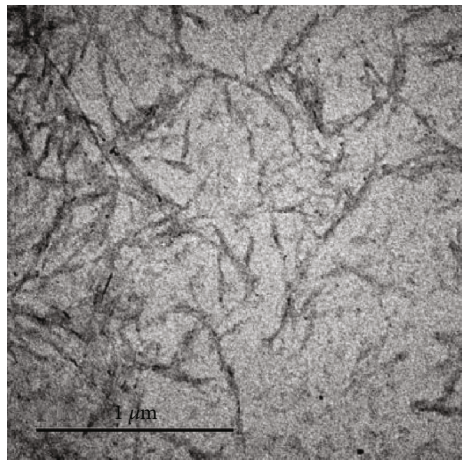

Figure 1: Micromorphology of CNCs.

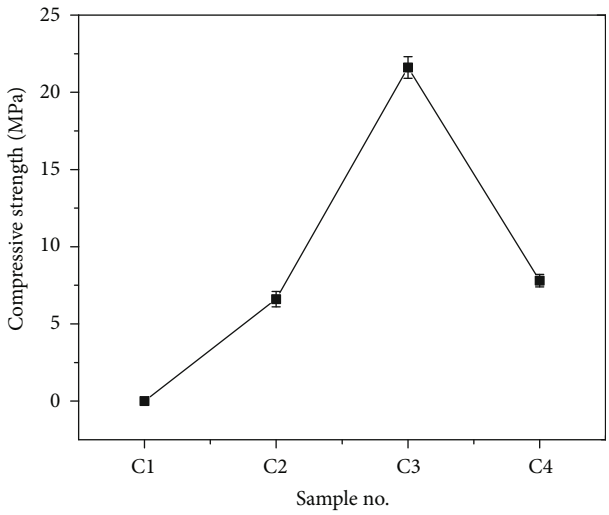

Figure 2: Effect of CNCs on compressive strength of cement pastes.

3. Results and Discussion

3.1. Micromorphology of CNCs. Figure 1 shows the micromorphology of CNCs in water. It is observed that CNCs are dispersed well in deionized water.

3.2. Mechanical Properties. Figure 2 shows the compressive strength of the cement pastes. The compressive strength of cement pastes without CNCs cannot be obtained because of the cracking destruction of specimens. Firstly, cement pastes

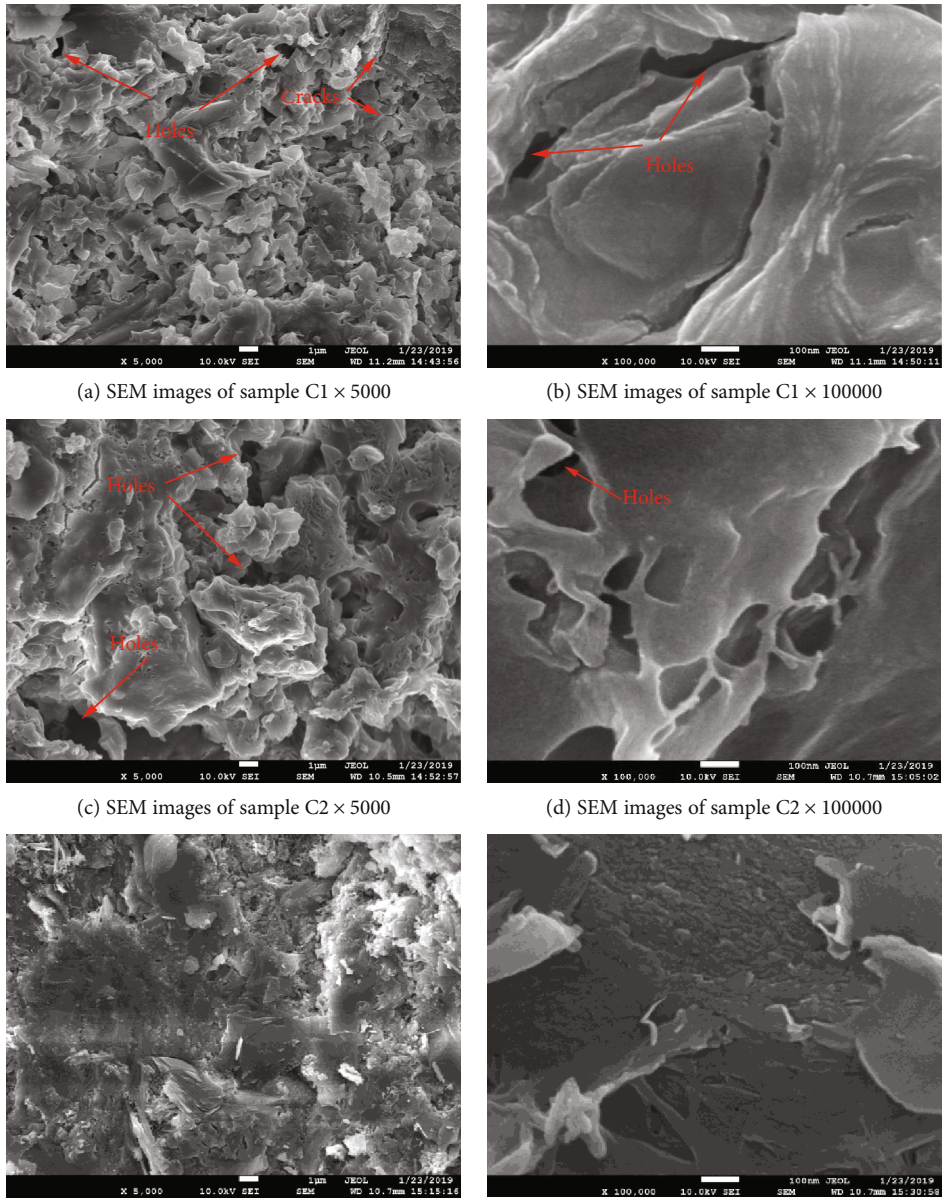

(a) SEM images of sample C1 × 5000

(b) SEM images of sample C1 × 100000

(c) SEM images of sample C2 × 5000

(d) SEM images of sample C2 × 100000

(e) SEM images of sample C3 × 5000

(f) SEM images of sample C3 × 100000

Figure 3: SEM images of samples C1, C2 and C3.

without aggregates have higher shrinkage and the higher water-cement ratio increases the shrinkage and brittleness of cement pastes. Secondly, the rapid decrease in temperature and humidity causes higher temperature and dry shrinkage deformation and worsens the hydration process of cement. Most surprisingly, it was found that a mere 0.5% CNCs addition could improve the mechanical properties of cement pastes significantly under the detrimental curing system. It was seen that CNC addition has excellent effect in preventing cement pastes from cracking. This notable result indicates that CNCs have exciting application prospects in concrete construction under lower temperatures, but not freezing environments.

3.3. Micrographs. In order to avoid the interference caused by the selected areas, several photos were taken with different magnifications in different zones of the cement pastes. The effect of CNC addition on the microstructure of cement pastes is very evident. Figures 3(a) and 3(b) show the SEM images of cement pastes without CNCs; Figures 3(c) and 3(d) show the SEM images of cement pastes with 0.2% CNCs; and Figures 3(e) and 3(f) show the SEM images of cement pastes with 0.5% CNCs. It is observed that the cement paste without CNCs has many gas holes and loosing structures. The microstructure of cement pastes is enhanced when CNCs are introduced into the samples. Figures 3(e)–3(f) show that 0.5% CNCs compact the cement paste and evidently reduce pores and cracks.

3.4. XCT. Figures 4(a) and 4(b), Figures 5(a) and 5(b), Figures 6(a) and 6(b), and Figures 7(a) and 7(b) show the 3D defect images of CNC/cement pastes with different

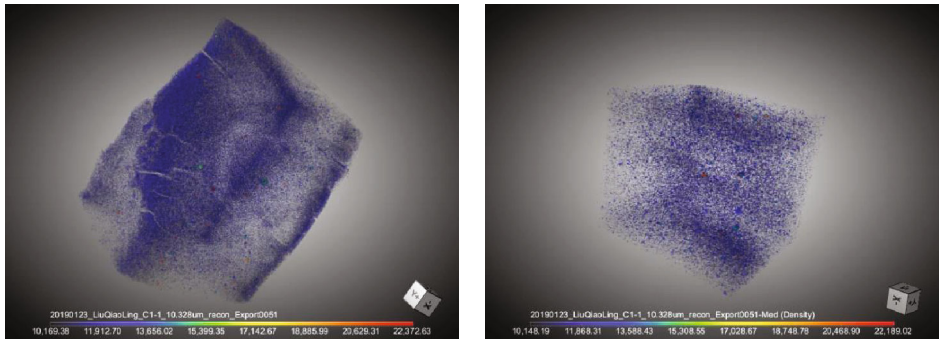

(a) Initial image (b) Cropped image

Figure 4: 3D images of sample C1 with 0.0% CNCs.

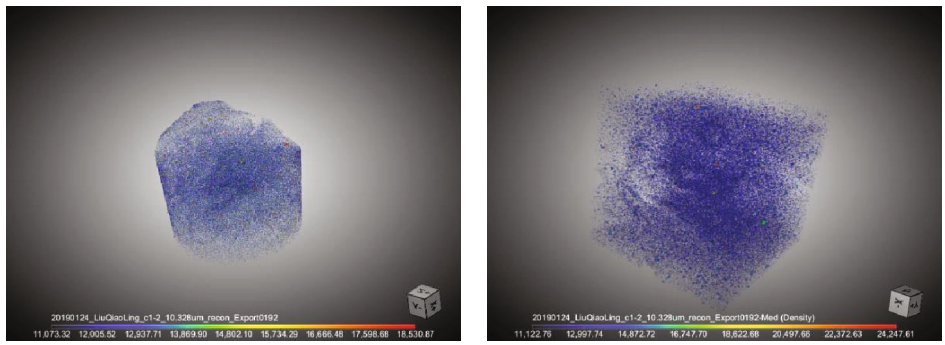

(a) Initial image (b) Cropped image

Figure 5: 3D images of sample C2 with 0.2% CNCs.

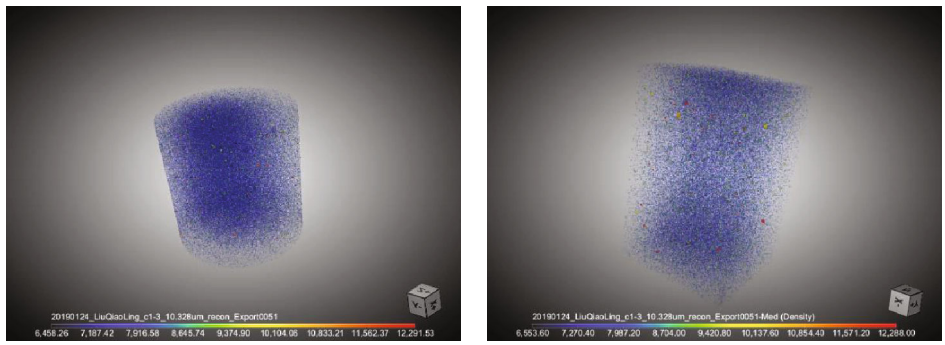

(a) Initial image (b) Cropped image

Figure 6: 3D images of sample C3 with 0.5% CNCs.

amounts of CNCs. Figure 8 shows the two-dimensional (2D) images of the defect segmentation. It is evident that the shape of sample C1 is irregular because it is so fragile that the central cylinders cannot be obtained with a water saw. A box has been cropped from the initial 3D images in order to avoid the boundary layer interaction. It is observed that the defects in sample C3 reduce; 0.5% CNC addition can improve the mesoscopic structure significantly under a detrimental environment.

In order to check the effect of CNCs on 3D defect distribution of cement pastes, the defect counts of the same volume (309, 550, 999, and 395.70 μm^3) were statistically studied. Figures 9(a) and 9(b) show the effect of CNCs on 3D defect distribution of cement pastes. Figures 9(a) and 9(b) show that the count of the total 3D defects reduces when CNCs are introduced into the cement pastes. When the amount of CNCs is 0.5% of cement by weight, the 3D defect count is the lowest between 1000 μm^3 and 10000 μm^3; however, the 3D defect count greater than 10000 μm^3 is slightly higher than that in sample C4. It is observed that CNCs play an important role in decreasing 3D defects between 1000 μm^3 and 10000 μm^3 of cement pastes.

3.5. Pore Size Analysis by Nitrogen Adsorption. Figure 10 shows the effect of the addition of CNCs on micropore and mesopore distribution in cement pastes. It is seen that sample C3 has the highest volume of pores between 0 and 250 nm. In comparison, Figure 10 shows that the count of 3D defects

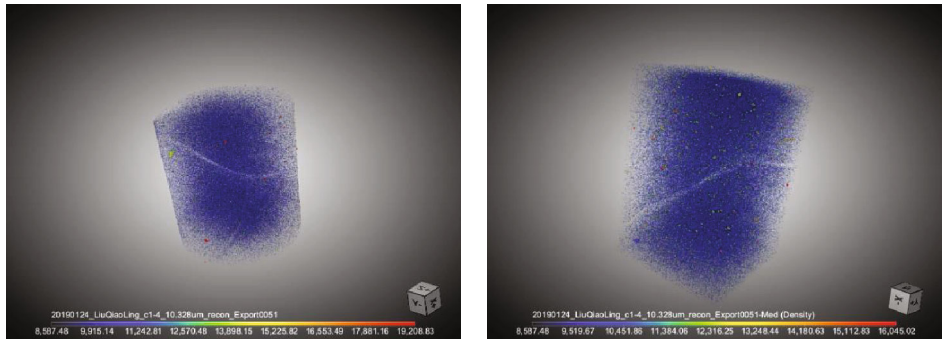

(a) Initial image (b) Cropped image

Figure 7: 3D images of sample C4 with 0.2% CNCs.

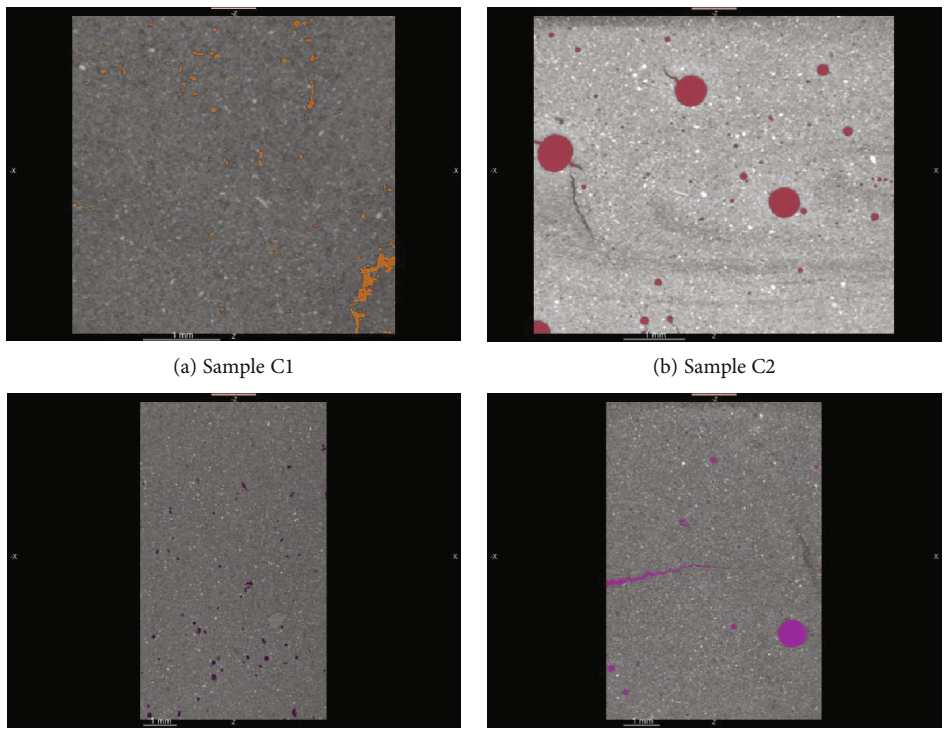

(a) Sample C1 (b) Sample C2

(c) Sample C3 (d) Sample C4

Figure 8: 2D images of the defect segmentation.

between 1000 and 10000 μm^3 (the pore size is approximately 10–20 μm) in sample C3 is the lowest. Thus, the addition of CNCs has a positive effect on the pore size distribution of cement pastes; this addition also leads to a pore structure refinement.

Furthermore, a very interesting discovery was made. In order to avoid the possibility of this being an accidental finding, repetitiveness of the nitrogen adsorption test was validated. It was found that 4–12 nm pores in sample C1, 3–7 nm pores in sample C2, and 3–8 nm pores in sample C4 disappeared.

Numerous studies show that there is no obvious separation between the C–S–H interlayer space width, gel pore width, and the sizes of interhydrate and capillary pores of cement pastes [17–20]. However, Valori et al. [21] and Muller et al. [22, 23] do define the interhydrate pore width in cement matrix and the size of the C–S–H interlayer space and gel pore size. The size of the pores that disappeared in sample C1 is in good agreement with the C–S–H interlayer space size, gel pore size, and interhydrate pore size obtained in their research results. When the CNC content is increased to 0.5% (sample C3), 3–10 nm pores appear completely. Figure 1 shows that the compressive strengths of samples C1 and C3 are 0 MPa and 21.6 ± 0.7 MPa, respectively. Therefore, almost no hydration products including C-S-H gel were formed in sample C1 under extreme conditions. The absence of 3–7(8) nm pores in samples C2 and C4 shows that almost no C-S-H gel is formed in those samples either. It is possible that a rapid decrease in temperature and humidity leads to a difficulty in the formation of CSH.

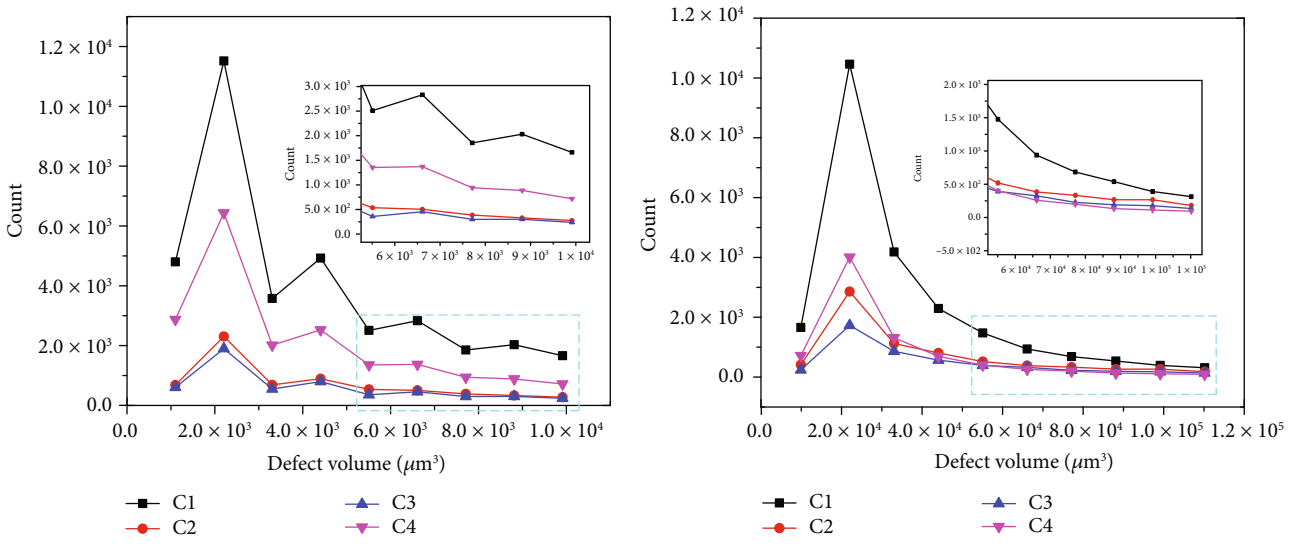

(a) 3D defect distribution

(b) 3D defect distribution

Figure 9: 3D defect distribution in cement pastes.

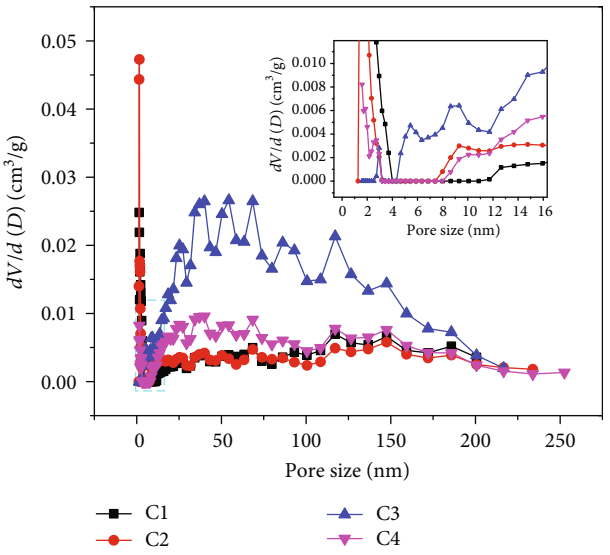

Figure 10: Pore size distribution in cement pastes.

4. Conclusions

The effect of the addition of CNCs on the properties of cement composites has been studied in this work. Encouragingly, we find that this addition can improve the properties of cement pastes significantly under the curing conditions defined when a rapid decrease in temperature and humidity occurs.

The pore distributions of cement pastes show that the addition of CNCs improves the microstructure of cement paste; the pore structure refinement in the cement matrix has happened. The nitrogen adsorption results show that almost no hydration products, including C-S-H gel, are formed in cement pastes without any addition of CNCs under extreme conditions. A rapid decrease in temperature and humidity leads to a difficulty in the formation of CSH.

The addition of CNCs has an excellent effect in promoting the hydration of cement and preventing cement pastes from cracking under extreme conditions. CNCs have potential application prospects in concrete construction under lower temperature but not in an environment that promotes freezing.

Data Availability

The data in our manuscript is available. The data used to support the findings of this study are included within the supplementary information file.

Conflicts of Interest

We declare that we do not have any commercial or associative interest that represents a conflict of interest in connection with the work submitted.

Acknowledgments

This work was supported by the National Natural Science Foundation of China (grant number 51608311); the Program for Changjiang Scholars and Innovative Research Team from the University of China (grant number IRT_17R69); and a Jiangsu Key Laboratory of Construction Materials Open Fund (grant number CM2016-07). We thank Editage (http://www.editage.cn) for its linguistic assistance during the preparation of this manuscript.

Supplementary Materials

The original figures are in the file of "Tiff". The original data of Fig.2, Fig.9 a, Fig.9 b and Fig.10 is in the file of "opj". The original nitrogen adsorption data of sample C1, C2, C3 and C4 are in the file of "nitrogen adsorption. *(Supplementary Materials)*

References

[1] L. Wang, J. Bao, L. Wang, F. Zhang, and Y. Li, "One-pot synthesis and bioapplication of amine-functionalized magnetite nanoparticles and hollow nanospheres," *Chemistry – A European Journal*, vol. 12, no. 24, pp. 6341–6347, 2006.

[2] K. Zhou, X. Wang, X. Sun, Q. Peng, and Y. Li, "Enhanced catalytic activity of ceria nanorods from well-defined reactive crystal planes," *Journal of Catalysis*, vol. 229, no. 1, pp. 206–212, 2005.

[3] S. Hu and X. Wang, "Ultrathin nanostructures: smaller size with new phenomena," *Chemical Society Review*, vol. 42, no. 12, pp. 5577–5594, 2013.

[4] Y. Long, J. Hui, P. Wang et al., "Hydrogen bond nanoscale networks showing switchable transport performance," *Scientific Reports*, vol. 2, pp. 612–617, 2012.

[5] L. Luo, P. Wang, D. Jing, and X. Wang, "Self-assembly of TiO_2 nanoparticles into chains, films and honeycomb networks," *CrystEngComm*, vol. 16, no. 8, pp. 1584–1591, 2014.

[6] F. Saleem, Z. Zhang, B. Xu, X. Xu, P. He, and X. Wang, "Ultrathin Pt–Cu nanosheets and nanocones," *Journal of the American Chemical Society*, vol. 135, no. 49, pp. 18304–18307, 2013.

[7] P. Wang, H. Sun, Y. Ji, W. Li, and X. Wang, "Three-dimensional assembly of single-layered MoS_2," *Advanced Materials*, vol. 26, no. 6, pp. 964–969, 2014.

[8] B. Xu, P. He, H. Liu, P. Wang, G. Zhou, and X. Wang, "A 1D/2D helical $CdS/ZnIn_2S_4$ nano-heterostructure," *Angewandte Chemie International Edition*, vol. 53, no. 9, pp. 2339–2343, 2014.

[9] K. Wang, Z. Zhang, X. Wang, and Y. Li, "Inorganic nanocrystals: from molecular design to systematic engineering," *Particuology*, vol. 17, pp. 1–10, 2014.

[10] P. N. Balaguru and S. P. Shah, *Fiber-Reinforced Cement Composites*, McGraw-Hill, New York, NY, USA, 1992.

[11] R. J. Moon, A. Martini, J. Nairn, J. Simonsen, and J. Youngblood, "Cellulose nanomaterials review: structure, properties and nanocomposites," *Chemical Society Reviews*, vol. 40, no. 7, pp. 3941–3994, 2011.

[12] J. E. Goodsell, R. J. Moon, A. Huizar, and R. B. Pipes, "A strategy for prediction of the elastic properties of epoxy-cellulose nanocrystal-reinforced fiber networks," *Nordic Pulp & Paper Research Journal*, vol. 29, no. 1, pp. 85–94, 2014.

[13] Y. Habibi and A. Dufresne, "Highly filled bionanocomposites from functionalized polysaccharide nanocrystals," *Biomacromolecules*, vol. 9, no. 7, pp. 1974–1980, 2008.

[14] Y. Habibi, L. A. Lucia, and O. J. Rojas, "Cellulose nanocrystals: chemistry, self-assembly, and applications," *Chemical Reviews*, vol. 110, no. 6, pp. 3479–3500, 2010.

[15] Y. Cao, P. D. Zavaterri, J. Youngblood, R. J. Moon, and J. Weiss, "The influence of cellulose nanocrystal additions on the performance of cement paste," *Cement and Concrete Composites*, vol. 56, pp. 73–83, 2015.

[16] Y. Cao, P. Zavattieri, J. Youngblood, R. Moon, and J. Weiss, "The relationship between cellulose nanocrystal dispersion and strength," *Construction and Building Materials*, vol. 119, pp. 71–79, 2016.

[17] H. M. Jennings, "A model for the microstructure of calcium silicate hydrate in cement paste," *Cement and Concrete Research*, vol. 30, pp. 101–116, 2000.

[18] H. M. Jennings, "Refinements to colloid model of C-S-H in cement: CM-II," *Cement and Concrete Research*, vol. 38, pp. 275–289, 2008.

[19] H. Roper, "Dimensional change and water sorption studies of cement paste," in *Symposium on structure of Portland cement paste and concrete*, pp. 74–83, Highway Research Board Special Report, Washington, DC, USA, 1966.

[20] M. Babaee and A. Castel, "Water vapor sorption isotherms, pore structure, and moisture transport characteristics of alkali-activated and Portland cement-based binders," *Cement and Concrete Research*, vol. 113, pp. 99–120, 2018.

[21] A. Valori, P. J. McDonald, and K. L. Scrivener, "The morphology of C–S–H: lessons from 1 H nuclear magnetic resonance relaxometry," *Cement and Concrete Research*, vol. 49, pp. 65–81, 2013.

[22] A. C. A. Muller, K. L. Scrivener, A. M. Gajewicz, and P. J. McDonald, "Use of bench-top NMR to measure the density, composition and desorption isotherm of C-S-H in cement paste," *Microporous and Mesoporous Materials*, vol. 178, pp. 99–103, 2013.

[23] A. C. A. Muller, K. L. Scrivener, A. M. Gajewicz, and P. J. McDonald, "Densification of C–S–H measured by ^{1}H NMR relaxometry," *The Journal of Physical Chemistry C*, vol. 117, pp. 403–412, 2013.